Spherical ion kinetic simulations of DT implosions

F. Vidal and J. P. Matte*
Institut National de la Recherche Scientifique–Énergie et Matériaux, 1650 Montée Ste-Julie, Case Postale 1020, Varennes, Québec, Canada J3X 1S2

M. Casanova and O. Larroche
Commissariat l'Énergie Atomique, Centre d'Études de Limeil–Valenton, 94195 Villeneuve–St.-Georges Cedex, France
(Received 7 October 1994)

The implosion of the DT plasma in an ablatively driven glass microballoon was simulated with a spherical ion kinetic code. The ion velocity distribution functions were strongly non-Maxwellian, and mostly depleted of fast ions. A high viscosity contributed to fuel heating, while large ion heat fluxes towards the pusher strongly cooled the fuel. This latter kinetic effect may explain in part why hydrodynamic simulations usually predict higher neutron yields than are measured.

PACS number(s): 52.50.Lp, 28.52.Cx, 52.25.Fi, 52.65.+z

During the past two decades, there has been steady progress towards inertial confinement fusion (ICF) [1–3]. In ICF, a glass or plastic microballoon containing deuterium-tritium (DT) fuel is symmetrically heated by an external energy source (intense laser beams, for example). The outer layers very rapidly expand outwards, and, due to the rocket effect, the inner ones (the "pusher") are driven inwards and they compress the fuel. Generally, experiments are simulated with hydrodynamic codes [3,4] which compute the time evolution of the density, velocity, and temperature, using the classical transport coefficients of Braginskii [5] for vicsosity and thermal conductivity (often with *ad hoc* limits), and assume Maxwellian velocity distribution functions to compute the rates of electron impact excitation and ionization as well as the rate of nuclear reactions in the DT fuel.

Very often, the measured neutron yield (Y_N) is much lower than that obtained from one dimensional (1D) hydrodynamic simulations [1–4,6–8], and deviations from spherical symmetry frequently explain much of this discrepancy. However, they cannot always fully account for it. For example, Richardson *et al.* [7] measured a yield of only 1.1×10^{11}, while their one dimension fluid simulation predicted 2.3×10^{12}, and a 2D simulation taking into account the illumination nonuniformity gave a prediction of 5×10^{11}. More recently, Bradley *et al.* [8] showed that beam smoothing greatly improves the situation, but still leaves the neutron yield considerably below that predicted by 1D fluid simulations. Therefore, it is necessary to investigate other mechanisms which tend to reduce Y_N, and we will see that ion kinetic effects might be a part of the explanation.

When gradient lengths are not much longer than the mean free path for Coulomb collisions, the above assumptions used in fluid codes are untenable [5], and corrections, better than mere limits on the transport terms, are needed. For steep electron temperature gradients, extensive kinetic simulations and theoretical studies have elucidated the modifications to the heat flow [9] and to the rates of ionization and excitation [10]. Recent studies of ion kinetic effects in planar shock waves [11–13] and in the collisional interaction of supersonic plasma streams [14,15] have shown highly anisotropic non-Maxwellian ion velocity distributions and very large viscous pressures and ion heat fluxes.

Braginskii viscosity is very small in cold, dense plasmas, and for this reason, it is often neglected in fluid codes, while an artificial viscosity is added to help numerical stability in shock propagation. However, for DT gas-filled glass microballoons, Braginskii viscosity turns out to be very important. Comparative fluid simulations by Yabe and Yanaka [4], with artificial viscosity and with Braginskii viscosity, showed that it helped to heat the DT fuel, and also inhibited compression. The predicted minimum fuel diameter was then closer to the measured value, but the higher ion temperature more than compensated for the effect of reduced compression on the predicted neutron yield which thus turned out to be even further above the measured value. However, these workers did not address the issue of ion heat flow in that article [4].

While the neutron yields we have found in our simulations are comparable, though somewhat lower than those computed in fluid simulations, the most noticeable qualitative aspect of the present work is the very large ion heat flow towards the pusher, which tends to cool the fuel. This is an effect which can contribute to the degradation of the neutron yield. It was also found that this large ion heat flow was enhanced by the very important viscosity effects.

Because of the Z^{-4} scaling of the mean free path for ion-ion Coulomb collision, ion kinetic effects are likely to be more important in the DT fuel than in the pusher. We address here three concerns for which there are, at best, only a few approximate calculations. In increasing order of importance, these are (a) the thermalization of the converging shock when it reaches the center [4]; (b) escape of the more energetic fuel ions, depleting the core of its more reactive ions [16,17]; and (c) fuel cooling by ion thermal conduction towards the pusher.

In this article, we present a first spherical, ion kinetic simulation of the dynamics of a DT plasma implosion,

*Author to whom correspondence should be addressed.

taking into account the full anisotropy in velocity space, as well as the dependence on radius and time. We have modeled the implosion of a thin (1.46 μm), 911 μm diameter, glass microballoon filled with DT gas at 3 atm, ablatively driven by a 8 kJ, 750 ps, 0.53 μm wavelength laser pulse, as in a recent ICF experiment reported by the Osaka group [4,18,19] for which several hydrodynamic simulations were performed [3,4]. This particular experiment, in which the fuel is imploded by multiplexing of strong shocks, was also chosen for our ion kinetic simulations because of its insensitivity to the initial temperature (T_0), which we set to 100 eV, instead of room temperature (0.025 eV). This made it possible for the velocity grid of the kinetic code to accommodate both T_0 and the temperatures of over 10 keV which occur at maximum compression. Insensitivity to T_0 was verified both by simulations of the experiment with the Limeil hydrodynamic code FCI1 [6], and by redoing our ion kinetic simulation with $T_0=200$ eV.

The time dependent position $R(t)$ and temperature $[T_e=T_i=T(t)]$ of the pusher-fuel interface were taken from a FCI1 simulation. In Fig. 1, we show this imposed $R(t)$, along with dY_N/dt, the volume integrated nuclear reaction rate, computed by the kinetic code as will be explained below. The time integral of this is the predicted neutron yield, Y_N, for which we obtained $Y_N=7\times10^{12}$, which is close to the values given by the current 1D hydrodynamic codes [3,4] and also above the measured value of 1.25×10^{12}. Plausible variations on the simulation conditions reduced the predicted Y_N to 3×10^{12}. Considering the various approximations made in our model, especially about the fuel-pusher interaction, it is not our goal here to make a close comparison of our results with those coming from experiments or purely hydrodynamic codes. We rather wished to set ourselves in reasonably realistic conditions to observe the departures of the ion distribution functions from equilibrium and consequences on the macroscopic scale.

The DT was modeled as a single ion species, of atomic mass 2.5, using our ion kinetic code "FPION" [12,13,15]. It advances in time the ion distribution function $F_i(r,v_r,v_\perp,t)$ while the electrons are treated as a fluid, assuming quasineutrality, and their temperature is computed using classical [5] heat flow, with Q_e limited to 0.1

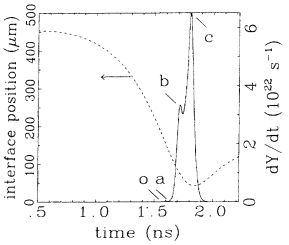

FIG. 1. Time evolution of the radius of the fuel-pusher interface (from the FCI1 hydrocode simulation), and of the neutron production rate from our kinetic simulation. The time integral gives the total neutron yield of 7×10^{12}. Marked times correspond to (*o*, 1.56 ns) propagating shock; (*a*, 1.62 ns) arrival of faster ions in the center and beginning of neutron production; (*b* 1.71 ns) arrival of the shock at the center and first peak of neutron production; (*c*, 1.81 ns) maximum compression and neutron production.

times the electron free streaming heat flow $Q_{eFS}=n_eT_e^{3/2}/m_e^{1/2}$, which is adequate because electron temperature gradients are not very steep [9]. The ion kinetic equation and the electron fluid, energy equation [Eqs. (1) and (2) in Ref. [12]] were adapted to spherical geometry. These are now, respectively,

$$\frac{\partial F_i}{\partial t}+v_r\frac{\partial F_i}{\partial r}+\frac{v_\perp^2}{r}\frac{\partial F_i}{\partial v_r}-\frac{v_rv_\perp}{r}\frac{\partial F_i}{\partial v_\perp}+\frac{eE_{\rm eff}}{m_i}\frac{\partial F_i}{\partial v_r}=(\partial F_i/\partial t)_{i-i}+(\partial F_i/\partial t)_{i-e}\ , \quad (1)$$

where $E_{\rm eff}$ is an effective electric field, given by the electron pressure gradient: $eE_{\rm eff}=(-1/n_i)\partial(n_ik_BT_e)/\partial r$. The other symbols have their usual meaning: t is time, r is the radial coordinate, v_r and $v_\perp$ are the radial and perpendicular velocity. The full anisotropy of the velocity distribution is retained in the kinetic equation as well as in the ion-ion collision operator (first term on the right), while ion-electron collisions (second term) are calculated to lowest order in $(m_e/m_i)^{1/2}$, assuming Maxwellian electrons:

$$\tfrac{3}{2}[(\partial T_e/\partial t)+u(\partial T_e/\partial r)]+T_e(1/r^2)(\partial/\partial r)(r^2u)=\frac{1}{n_i}\frac{1}{r^2}\frac{\partial}{\partial r}(r^2Q_e)+3\frac{m_e}{m_i}\tau_{ei}^{-1}(T_e-T_i)\ , \quad (2)$$

where u is the mean ion velocity. The computational cells are of uniform size, but they contract or expand, so that $Nr\Delta r(t)=R(t)$ [the extra terms in the kinetic equation which account for this moving grid are not displayed in Eqs. (1) and (2), for clarity]. The boundary condition at the origin is reflecting: $T_e(-r,t)=T_e(r,t)$; $F_i(-r,v_r,v_\perp,t)=F_i(r,-v_r,v_\perp,t)$. The boundary condition at the pusher-fuel interface involves some degree of uncertainty due to the lack of knowledge about the interaction between the pusher and the fuel on the atomic scale. We chose to reemit the incident fuel ions as a Maxwellian at the (imposed) interface temperature. This is consistent with the assumption usually made in Lagrangian hydrodynamic codes that there is heat flow, but no diffusion of material across the interface. We will discuss later modifications to this boundary condition.

Macroscopic quantities are plotted in Fig. 2, at the four times indicated on Fig. 1. These ionic quantities are obtained from the distribution functions in the usual way [20]: the temperature, heat flux, and pressure tensor are calculated in the local rest frame of reference, i.e., the local mean ion velocity is zero.

At time "*o*" towards the end of the acceleration phase, the density and temperature are relatively modest, but both the normalized viscous pressure and the ion heat flux reach very high values: this highly directional motion of the ions streaming towards the center is even more pronounced than that seen in planar shock simulations [12,13]. At time "*a*", the first fast ions have passed the center. Due to spherical geometry, their motion is now primarily perpendicular to the radius, so that the viscous pressure is negative, and the normalized heat flow is small. This is seen in Fig. 3(a), left, which displays a velocity space contour plot of $F_i(r,v_r,v_\perp,t)$ at this time, at a position fairly near the center: there is the original, nearly unperturbed plasma, at low velocity, and the fast

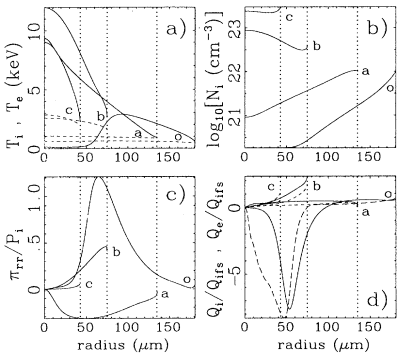

FIG. 2. Profiles of macroscopic quantities at the four different times indicated on Fig. 1. Vertical dashed lines indicate the radius of the fuel at the three later times. (a) Ion and electron temperature (full and dashed lines, respectively); (b) density; (c) ratio of viscous ion pressure to the usual $P_i = N_i k_B T_i$; (d) ratio of ion and electron heat flow to the local ion streaming value $Q_{ifs} = N_i (k_B T_i)^{3/2} m_i^{-1/2}$ (full and dashed lines, respectively).

ions whose ballistic motion is apparent. At the right, Fig. 3(a'), we have plotted the energy distribution function (there is a dip near the origin because the mean velocity falls in a depopulated region of velocity space), and the Maxwellian at the same density and temperature. At these earlier times "*o*" and "*a*", the density and temperature [Figs. 2(a) and 2(b)] are too low for significant nuclear reactivity, which is far more important at times "*b*" and "*c*", as can be seen in Fig. 1. At these times, the density and temperature are much higher, and faster ions stream towards the pusher. Close to it, this streaming motion is clearly evident [Fig. 3(b)], and it implies a surplus of fast ions compared to the local Maxwellian

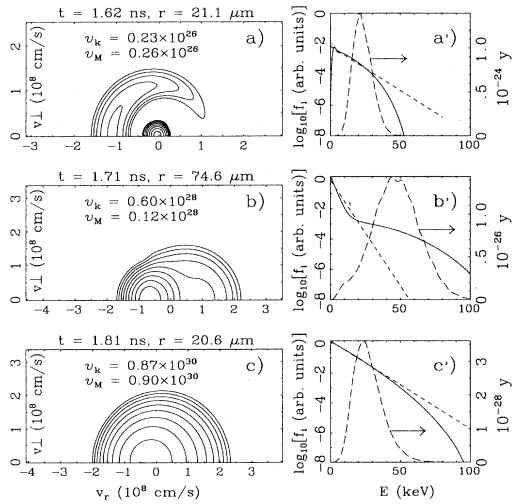

FIG. 3. Left: Velocity space contour plots (with a $10^{-1/2}$ factor between contours); Right: Energy distribution and Maxwellian at the same density and temperature (full and short dashed lines), and contribution to the reaction rate (in $cm^{-3}\,s^{-1}\,keV^{-1}$, long dashed lines), as explained in the text. Note that the scales for *y* differ. The times (corresponding to those indicated in Fig. 1) and radial position are indicated for each. Also given are v_k, the reaction rate from the actual distribution function, and v_M, that from a Maxwellian at the same density and temperature. The densities (in 10^{21} cm^{-3}) and temperatures (in keV) are, respectively, (a) 1.18,7.5; (b) 34.8,3.1; (c) 225.3,7.4.

[Fig. 3(b')]. The ion heat flux is even higher than the electron heat flux there [Fig. 2(d), curve *b*]. Cooling of the plasma by ion thermal conduction is a very important effect, even more than could have been obtained from usual fluid models, because Q_i is often higher than Q_{ifs}. We find that the time integrated energy loss due to ion heat flow to the pusher is equal to the electron heat flow loss, but the ionic loss which peaks at 1.75 ns, shortly before the maximum neutron production (1.81 ns, see Fig. 1) is more damaging to the yield than the electron heat loss, which peaks slightly after, at 1.82 ns. The factor of $(m_e/m_i)^{1/2}$ in the ratio of the Braginskii thermal conductivities is overcome both by the slightly higher ion temperature and the large viscosity effects, which make the ions' radial velocities higher than the perpendicular ones, and thus enhance the value of Q_i/Q_{ifs}. Closer to the center, for example, at approximately $R(t)/2$, Fig. 3(c), there is some anisotropy, corresponding to considerable outward heat flow [Fig. 2(d), curve *c*], but the distribution function is depleted of its fast ions [above 40 keV, in Fig. 3(c')]. This is representative of regions which contribute most to the neutron yield. The large ion heat flow keeps the ion temperature profiles rather peaked at the center [Fig. 2(d), curves *b* and *c*], which is an important difference from hydrodynamic simulations, which frequently show a flat ion temperature profile, with a sudden fall at the pusher (as in Fig. 3 of Ref. [3]).

To assess the effect of the depletion of the tail of the ion energy distribution on the neutron yield, which is the third issue addressed in this paper, we computed the neutron production rate per unit volume, $v_k(r,t) = (\frac{1}{4}) \int d^3\mathbf{v} \int d^3\mathbf{v}' |\mathbf{v}-\mathbf{v}'| \sigma(|\mathbf{v}-\mathbf{v}'|) F_i(r,\mathbf{v},t) F_i(r,\mathbf{v}',t)$, and compared it to $v_M(r,t)$, obtained if $F_i(r,\mathbf{v},t)$ were a Maxwellian of equal density and temperature. The calculation of v_k, which is computationally expensive, was done only for several positions and times, and the reaction rate plotted in Fig. 1 is a volume integral of v_M. The DT fusion cross section is taken from Ref. [21]. Where the reactivity is important [of which Figs. 3(c) and 3(c') are typical] we have found that v_k is only slightly less than v_M (both are printed on Fig. 3 for all three points indicated there). To understand this behavior, we evaluated $v_k(r,t,E)$, i.e., $v_k(r,t)$ but with the velocity integrals restricted to $|\mathbf{v}|, |\mathbf{v}'| < (2E/m_i)^{1/2}$, and evaluated the contribution of each energy increment $y(r,t,E) = dv_k(r,t,E)/dE$, which is plotted in Fig. 3 (long dashed lines). The main contribution to the rate is from ions of energy 15–30 keV, while the depletion is significant only above 40 keV [Fig. 3(c')], which explains why v_k is only slightly less than v_M. The opposite is true close to the pusher [Fig. 3(b')]: v_k is five times higher than v_M, due to the faster ions which are streaming towards the nearby pusher and their contribution dominates that of the bulk; but this behavior, while interesting in itself, does not contribute much to the global yield because the v_k of Fig. 3(b) is two orders of magnitude lower than that of Fig. 3(c), and at time "*b*", for points farther from the pusher, the behavior is much like that in Fig. 3(c).

Variations on the pusher trajectory and pusher-fuel boundary condition were made. The imposed minimum

fuel radius of 40 μm was based on the FCI1 fluid simulation, and was equal to Atzeni's (Fig. 3 of Ref. [3]) and close to that of Yabe and Tanaka, when they applied the usual artificial viscosity [4]. We performed another ion kinetic simulation in which the imposed pusher trajectory had a minimum radius of 55 μm, as computed in their fluid simulation with Braginskii viscosity, and closer to the measured value [4]. This gave rather similar fuel dynamics and temperatures, but the neutron yield was reduced from 7×10^{12} to 3×10^{12}, simply due to the lesser compression. We conclude that varying the imposed pusher trajectory, within some reasonable limits, does not qualitatively affect our results. Reverting to the standard pusher trajectory (40 μm minimum radius), we made two variations on the boundary conditions. In the first one, the fuel ions impinging on the pusher were partially absorbed, so that, by the end of the simulation, one-third of all ions had been lost. This had modest effects on the ion temperature, etc., but the neutron yield was reduced to 3×10^{12}, due to the lower density. On the contrary, when a perfectly reflective boundary condition at the pusher-fuel interface was used (for both ions and electrons), not only were the temperatures higher, increasing and neutron yield tenfold, but also, the distributions had an excess of fast ions due to frequent rebounds on the shell. Such a condition is clearly unrealistic, but these tests underscore the importance of the fuel-pusher boundary condition, a topic which perhaps deserves more attention than it has received to date.

In summary, we have simulated the implosion of the DT fuel in an ablatively driven glass microballoon target with an ion kinetic code describing the fuel, with the pusher trajectory and temperatures being taken from an independent fluid simulation. Our model fits the available experimental data, for the case considered here, at least as well as the current hydrodynamic codes. The ion velocity distributions are highly non-Maxwellian and anisotropic, thus raising doubts on the validity of the usual approximations of fluid modelling. Surprisingly, the local nuclear reactivities are almost equal to those calculated with a Maxwellian at the same density and temperature, where these are important. Most importantly, ion heat flow towards the pusher cools the fuel ions considerably, and equals electron heat flow in terms of energy loss. This ion heat flow is enhanced by the large positive viscous pressure which contributes to fuel heating. Different pusher trajectories leave these conclusions essentially unchanged.

To improve the kinetic model, it would be necessary to (1) investigate the fuel-pusher interaction on the atomic scale in order to improve the boundary condition of the fuel distribution function at the interface, a task which could be carried out by means of a kinetic model designed to take into account simultaneously the pusher ions and the fuel ions, and (2) couple consistently the kinetic simulation of the fuel to the pusher's motion and temperature (obtained from a fluid code, for instance), and it can be expected that the compression would indeed be reduced due to the large viscous pressure near the interface seen in the kinetic simulation, but not included in the fluid one.

In high gain cryogenic targets, a central hot spot of a size roughly comparable to that of the entire fuel in the present study is surrounded by cold fuel which compresses the center, somewhat as the pusher compresses the fuel [2] in smaller targets, except that the hot ions are more likely to be lost for the hot spot rather than merely thermalized (due to the Z^{-2} scaling of their mean free path). Although the peak density reached in such targets is about one order of magnitude greater than that obtained here, thus reducing considerably the ion mean free path, one can expect from our results that fast ions would hinder the formation of the hot spot by evacuating heat from the center at a rate higher than expected from usual fluid models. To simulate this, new methods would be required, such as a hybrid model with a cold fluid plus hot kinetic ions, to avoid a prohibitively large velocity grid. Our results underscore the need for a better model of ion heat flow and viscosity in hydrodynamic codes, analogous to the improved models for electron heat flow [9].

This work was supported in part by the Ministère de l'Éducation de Québec and by a strategic grant from the Natural Sciences and Engineering Research Council of Canada. Useful discussions with Dr. J. Virmont, Dr. T. W. Johnston, Dr. P. Drake, and Dr. M. D. Rosen are gratefully acknowledged.

[1] R. L. McCrory and J. M. Soures, in *Laser-Induced Plasmas and Applications,* edited by L. J. Radziemski and D. A. Cremers (Dekker, New York, 1989), p. 207.
[2] J. D. Lindl, in *Inertial Confinement Fusion,* edited by A. Caruso and E. Sindoni (Editrice Compositore, Bologna, 1988), pp. 587 and 617.
[3] S. Atzeni, Plasma Phys. Contr. Fusion **29**, 1535 (1987).
[4] T. Yabe and K. A. Tanaka, Laser Part. Beams **7**, 259 (1989).
[5] S. I. Braginskii, in *Reviews of Plasma Physics,* edited by M. A. Leontovich (Consultants Bureau, New York, 1965), Vol. 1, p. 205.
[6] C. Bayer *et al.*, Nucl. Fusion **24**, 573 (1984).
[7] M. C. Richardson *et al.*, Phys. Rev. Lett. **56**, 2048 (1986).
[8] D. K. Bradley *et al.*, Phys. Rev. Lett. **68**, 2774 (1992).
[9] Review in J. Delettrez, Can. J. Phys. **64**, 932 (1986).
[10] J. P. Matte *et al.*, Phys. Rev. Lett. **72**, 1208 (1994).
[11] K. Abe and G. Sakaguchi, Phys. Fluids **28**, 3581 (1985).
[12] M. Casanova *et al.*, Phys. Rev. Lett. **67**, 2143 (1991).
[13] F. Vidal *et al.*, Phys. Fluids B **5**, 3182 (1993).
[14] S. M. Pollaine *et al.*, Phys. Fluids B **4**, 989 (1992).
[15] O. Larroche, Phys. Fluids B **5**, 2816 (1993).
[16] A. G. Petschek and D. B. Henderson, Nucl. Fusion **19**, 1678 (1979).
[17] T. Nishikawa, H. Takabe, and K. Mima, Jpn. J. Appl. Phys. **28**, 2004 (1989).
[18] C. Yamanaka *et al.*, Phys. Rev. Lett. **56**, 1575 (1986).
[19] H. Takabe *et al.*, Phys. Fluids **31**, 2884 (1988).
[20] N. A. Krall and A. W. Trivelpiece, *Principles of Plasma Physics* (McGraw-Hill, New York, 1973), pp. 78–88.
[21] David L. Book, *NRL Plasma Formulary,* Naval Research Laboratory Publication No. 177-4405, 1990, p. 44–45.